

Solar tachocline dynamics: eddy viscosity, anti-friction, or something in between?

MICHAEL E. McINTYRE

Centre for Atmospheric Science[†] at the
Department of Applied Mathematics and Theoretical Physics,
Centre for Mathematical Sciences,
Wilberforce Road,
Cambridge CB3 0WA, UK
<http://www.atm.damtp.cam.ac.uk/people/mem/>

Invited paper to appear as chapter 8 in

Stellar Astrophysical Fluid Dynamics

a Festschrift in honour of Douglas Gough
on the occasion of his 60th birthday

ed. M.J. Thompson & J. Christensen-Dalsgaard
Cambridge, University Press, pp. 111–130, in press for 2003.

[†] The Centre for Atmospheric Science is a joint initiative of the Department of Chemistry and the Department of Applied Mathematics and Theoretical Physics (<http://www.atm.damtp.cam.ac.uk/>).

8

Solar tachocline dynamics: eddy viscosity, anti-friction, or something in between?

MICHAEL E. McINTYRE

*Centre for Atmospheric Science at the
Department of Applied Mathematics and Theoretical Physics,
Centre for Mathematical Sciences, Wilberforce Road, Cambridge CB3 0WA, UK,
<http://www.atm.damtp.cam.ac.uk/people/mem/>*

The tachocline has values of the stratification or buoyancy frequency N two or more orders of magnitude greater than the Coriolis frequency. In this and other respects it is very like the Earth's atmosphere, viewed globally, except that the Earth's solid surface is replaced by an abrupt, magnetically-constrained 'tachopause' (Gough & McIntyre 1998). The tachocline is helium-poor through fast ventilation from above, down to the tachopause, on timescales of only a few million years. The corresponding sound-speed anomaly fits helioseismic data with a tachocline thickness $(0.019 \pm 0.001)R_{\odot}$, about 0.13×10^5 km (Elliott & Gough 1999), implying large values of the gradient Richardson number such that stratification dominates vertical shear even more strongly than in the Earth's stratosphere, as earlier postulated by Spiegel & Zahn (1992). Therefore the tachocline ventilation circulation cannot be driven by vertically-transmitted frictional torques, any more than the ozone-transporting circulation and differential rotation of the Earth's stratosphere can thus be driven. Rather, the tachocline circulation must be driven mainly by the Reynolds and Maxwell stresses interior to the convection zone, through a gyroscopic pumping action and the downward-burrowing response to it. If layerwise-two-dimensional turbulence is important, then because of its potential-vorticity-transporting properties the effect will be anti-frictional rather than eddy-viscosity-like. In order to correctly predict the differential rotation of the Sun's convection zone, even qualitatively, a convection-zone model must be fully coupled to a tachocline model.

8.1 Introduction

In the quintessential Douglas Gough manner I am going to be provocative straight off and say, in answer to the question in the title, that 'anti-friction' is closer to the mark – flying in the face of classical turbulence theories.

How can I make such an outrageous assertion? I can do so because in significant respects the Sun’s interior is very like the Earth’s atmosphere, and we observe the Earth’s atmosphere doing it all the time, that is, showing anti-frictional behaviour. By ‘anti-frictional’ I mean that if we describe the fluid system in terms of a differentially-rotating mean state with angular velocity $\bar{\Omega}(r, \theta, t)$ and azimuthal velocity $\bar{v}_\phi = r \sin \theta \bar{\Omega}(r, \theta, t)$, where r, θ, ϕ are radius, colatitude, and longitude and t is time, plus chaotic fluctuations \mathbf{v}' about that state, then the averaged effect of the fluctuations is to drive the system away from solid rotation.

This of course contradicts the classical idea, enshrined in the term ‘eddy viscosity’, that chaotic fluctuations by themselves should drive, or rather relax, the system *toward* solid rotation. The attractiveness of that classical idea illustrates the perils of conflating ‘chaos’ with ‘turbulence’. The idea would be correct if another classical idea were correct, namely that turbulence theory should be like gas-kinetic theory, with the turbulent fluctuations acting like molecular-scale fluctuations about a nearly homogeneous mean state. Thus the gas-kinetic mean free path is replaced by some ‘mixing length’, ‘Austausch length’, or other lengthscale representative of the irreversible fluctuating displacements of fluid elements. That lengthscale may or may not be hidden from view within the complexities of a turbulence theory based on ‘closure’. If momentum is transported by the fluctuating displacements, and if typical displacements are much smaller than the scales of variation of the mean state – as implied by the stipulation ‘nearly homogeneous’ – then the effect of the fluctuations on the mean state is like that of a viscosity, relaxing the system toward solid rotation, essentially because of the scale separation just mentioned and the implied flux–gradient relations.

The recognition that fluctuations in the Earth’s atmosphere often do the opposite, *i.e.* drive the system away from solid rotation (though not, of course, arbitrarily far away), was a major paradigm shift within the terrestrial atmospheric sciences over the past century. That paradigm shift had its beginnings in the work of Harold Jeffreys in the second and third decades of the century (*e.g.* Jeffreys 1933[†]). It gathered pace in the late 1960s, stimulated by an increasing wealth of observational evidence. It was fundamental

[†] This conference paper, originally from *Procès-Verbaux de l’Assoc. de Météorol.*, UGGI, Lisbon, Part II (Mémoires), lucidly and cogently summarizes Jeffreys’ classic argument, developed over the preceding decade or more, that observed surface winds imply the existence of what Victor Starr later called the ‘negative viscosity’ due to the large-scale eddies, the cyclones and anticyclones, appearing on weather maps. The reported conference discussion (Jeffreys, *op. cit.*, pp. 210–11) illustrates that in 1933 no-one, not even Jeffreys, had the faintest idea of what kind of fluid dynamics might be involved. The ‘negative viscosity’ phenomenon was still flagged as a major enigma in the closing pages of the landmark review by E. N. Lorenz (1967).

to solving some of the greatest enigmas with which the atmospheric sciences were confronted in the 1960s.

One of those enigmas was the behaviour of $\bar{\Omega}(r, \theta, t)$ in the tropical stratosphere between 15–30 km, in which the sign of $\partial\bar{\Omega}/\partial r$ reverses quasi-periodically with a mean period around 27 months. This surprising phenomenon was first revealed by radiosonde balloon observations, which had become routine after the second world war in support of operational weather forecasting. The phenomenon is known today as the quasi-biennial oscillation or QBO. Its cause was wholly mysterious in the 1960s. Today, however, the QBO is recognized as one of the clearest illustrations of the point I am emphasizing, the tendency of chaotic fluctuations to drive a stratified fluid system, very often, away from solid rotation; and a further and even clearer illustration can be found in the beautiful laboratory experiment devised and carried out by Plumb & McEwan (1978). A stratified fluid in a large annulus is driven away from solid rotation, $\bar{\Omega} \equiv 0$ in this case, by nothing but the imposition of fluctuations via an oscillating boundary. On a timescale of many boundary oscillations, $\bar{\Omega}$ evolves away from zero, and then develops a pattern of reversals very like that of the QBO.

Together with appropriate conceptual and numerical modelling, the results from the Plumb–McEwan experiment have greatly illuminated our thinking about the QBO, and enriched our repertoire of models of it. The reader interested in the observed phenomena and in today’s understanding of them, which is secure, at least qualitatively – and in the history of ideas leading to that understanding – may consult my recent reviews (2000, 2002) together with a major review of research on the QBO by Baldwin *et al.* (2001), which latter includes an extensive discussion of the observational evidence. Movies of the Plumb–McEwan experiment plus ‘technical tips’ on how to repeat it are available on the Internet.†

8.2 Long-range and short-range momentum transport

How can the classical turbulence theories be so completely wrong, not just quantitatively but also qualitatively? The answer is not only clear with hindsight but also simple. Because the Earth’s atmosphere and the Sun’s interior are heavily-stratified, rotating fluid systems, the fluctuations, chaotic though they may be, inevitably feel the wave propagation mechanisms associated with rotation and stratification.

These include the propagation mechanisms of internal gravity waves, Coriolis or ‘inertial’ (epicyclic) waves, and layerwise-two-dimensional Rossby or

† at http://www.gfd-dennou.org/library/gfd_exp/exp-e/exp/bo/

vorticity waves. By its very nature, any wave propagation mechanism promotes systematic correlations among the fluctuating fields \mathbf{v}' , etc. Almost inevitably, the upshot is that momentum and angular momentum are transported over distances far greater than mixing lengths, limited only by the distances over which waves can propagate. Internal gravity waves provide a well known example, in which the most significant correlations are those between the horizontal and vertical components of \mathbf{v}' .

Of course there are exceptional cases in which the momentum transports exactly cancel, such as perfect g modes and p modes, in the strict sense of global eigenmodes subject to no excitation or dissipation. The cancellation is not trivial to demonstrate, when $\bar{\Omega} \neq 0$, but it can be demonstrated from the so-called ‘nonacceleration theorem’ of wave–mean interaction theory (*e.g.* McIntyre 2000 & refs.), essentially a consequence Kelvin’s circulation theorem applied around all latitude circles.

Long-range momentum transports of the kind in question are sometimes called radiation stresses (*e.g.* Brillouin 1925, on ‘tensions de radiation’). They are usually anisotropic, contrary to what might be suggested by the older term ‘radiation pressure’ still found in the literature. They are related to mean gradients in ways that are anything but local, the global eigenmodes being an extreme case. It is crucial to consider large-scale wavefields and the processes of generation, dissipation, refraction, Doppler-shifting, internal reflection, focusing and defocusing that shape the wavefields.

Classical turbulence theories – all the way from simplistic mixing-length theories to complicated closure theories – take no account of such long-range momentum-transport mechanisms. As already emphasized, the only momentum transport they consider is, by assumption, that arising from local, short-range, Austausch or material-exchange types of process. It is exactly that short-range character, and the implied or hoped-for scale separation, that give rise to ‘turbulent stresses’ involving flux–gradient relations and eddy viscosities. We may summarize what happens in the Earth’s atmosphere by saying that, on a global scale, radiation stresses dominate turbulent stresses. We shall see nevertheless that turbulence can be important in another way, namely through its contribution to shaping the wavefields, as with surf near ocean beaches.

8.3 Potential vorticity

Anti-frictional behaviour is not inevitable when radiation stresses dominate turbulent stresses, but experience has shown it to be commonplace. For instance such behaviour is often produced by broadband internal gravity

wave fields – broadband in the sense of having a range of horizontal phase speeds – like those generated by the Sun’s convection zone or by the Earth’s tropical thunderstorms. In fact the Plumb–McEwan experiment, in which the significant waves are internal gravity waves, shows that even two distinct horizontal phase speeds can be enough.

Anti-frictional behaviour is commonplace, too, in the case of Rossby-wave fields, whether broadband or not, for quite different reasons connected with the properties of the Rossby–Ertel potential vorticity, hereafter ‘PV’. Anti-frictional behaviour is especially characteristic of the stresses exerted horizontally by fluctuating layerwise-two-dimensional motion. That is why Gough & McIntyre (1998 & refs., hereafter GM) argued against horizontal eddy viscosity as explaining the thinness of the tachocline.

The PV, denoted here by the symbol Q , is a quantity central to the dynamics of heavily stratified fluid systems, including the dynamics of Rossby waves and other nearly-horizontal, layerwise-two-dimensional motions. Such other motions include layerwise-two-dimensional turbulence, also loosely called ‘geostrophic’ turbulence despite its possible existence near the equator. The properties of Q will expose the fact that such turbulence is itself intimately bound up with the Rossby-wave mechanism. This will be demonstrated in Sections 8.4 and 8.5. In the dynamical regimes under discussion there is no such thing as turbulence without waves.

In a reference frame rotating with angular velocity Ω_0 the PV, Q , is defined as

$$Q = \rho^{-1} (2\Omega_0 + \nabla \times \mathbf{v}) \cdot \nabla \vartheta , \quad (8.1)$$

where ρ is mass density and ϑ is potential temperature (materially invariant, $D\vartheta/Dt = 0$, for adiabatic motion; in place of ϑ one may equally well use specific entropy, or any other monotonic function of ϑ alone). For definiteness we identify Ω_0 with the angular velocity of the Sun’s interior just below the tachocline, $|\Omega_0| \approx 0.27 \times 10^{-5} \text{ rad s}^{-1}$ or 430 nHz, and take the axis of coordinates parallel to Ω_0 . Heavy stratification means that $\nabla \vartheta$ is nearly vertical, $\nabla \vartheta \approx \hat{\mathbf{r}} \partial \vartheta / \partial r$, where $\hat{\mathbf{r}}$ is a unit vertical (radial) vector. Heavy stratification also means that the associated buoyancy frequency N greatly exceeds the other reciprocal timescales of interest, including $|\Omega_0|$ and the vertical shear $r \sin \theta \partial \bar{\Omega} / \partial r$. We recall that N is defined by

$$N^2 = g \vartheta^{-1} \partial \vartheta / \partial r = g \partial (\ln \vartheta) / \partial r , \quad (8.2)$$

g being the local gravitational acceleration, and that the value of N is of the order of $10^{-3} \text{ rad s}^{-1}$ near the base of the tachocline. The standard measure of stratification against vertical shear, the gradient Richardson number, is

defined by

$$Ri = N^2(r \sin \theta \partial \bar{\Omega} / \partial r)^{-2}. \quad (8.3)$$

If we use the refined estimate of tachocline depth Δr obtained by Elliott & Gough (1999), $(0.019 \pm 0.001)R_\odot$, about 0.13×10^5 km, then typical vertical shears $\Delta \bar{v}_\phi / \Delta r \lesssim 10^{-5} \text{ s}^{-1}$, not much greater than $|\Omega_0|$. Thus $Ri \gtrsim 10^{-6} / 10^{-10} \sim 10^4 \gg 1$ near the base of the tachocline. Even when N is taken to be an order of magnitude smaller, $10^{-4} \text{ rad s}^{-1}$, as near the top of the tachocline, we still have $Ri \gtrsim 10^2 \gg 1$. This says that the tachocline is even more heavily stratified than the most heavily stratified portion of the Earth's stratosphere, where typically $Ri \gtrsim 10$ in a coarse-grain view.

Such Ri values are high enough to enforce layerwise-two-dimensional motion, everywhere including the equator, as pointed out by Spiegel & Zahn (1992, hereafter SZ). A key property of Q during such motion is that not only ϑ but also Q itself is materially invariant, $DQ/Dt \approx 0$, if the motion can be considered inviscid as well as adiabatic and if MHD (Lorentz) forces can be neglected within the tachocline. Approximately inviscid motion is consistent with large Ri values.†

A second key property of Q , which holds for any motion whatever – even a motion that feels MHD forces – is the integral relation

$$\iint_{\mathcal{S}} Q b \, dA = 0, \quad (8.4)$$

where dA is the surface area element and where the integral is taken globally over a stratification or isentropic surface \mathcal{S} , on which ϑ is constant by definition. The weighting factor $b = \rho / |\nabla \vartheta|$, a positive-definite quantity. It is a stratification-related mass density in the sense that $b \, d\vartheta$ is the mass per unit area between neighbouring stratification surfaces \mathcal{S} ; that is, $b \, dA \, d\vartheta$ is the mass element. The relation (8.4) is an immediate consequence of Stokes' theorem, the definition of Q , and the fact that each surface \mathcal{S} is topologically spherical and has no boundary. For present purposes both the Sun and the Earth are rapidly rotating bodies, with strongly polarized Q fields: except near the equator, $2\Omega_0$ dominates $\nabla \times \mathbf{v}$ in (8.1). So (8.4) is satisfied through

† Note also that tachocline thermal diffusion times estimated as $(\pi^{-1} \Delta r)^2 / \kappa$, where the thermal diffusivity $\kappa \sim 10^7 \text{ cm}^2 \text{ s}^{-1}$, come out at about 500y. This is well in excess of the likely timescales of months to years for any layerwise-two-dimensional motion that might occur in the tachocline. Viscous and magnetic diffusion times are far longer still. The inviscid, adiabatic material invariance of Q (Ertel's theorem) is easy to verify from $\nabla(D\vartheta/Dt) = 0$ together with the scalar product of $\nabla \vartheta$ with the inviscid, adiabatic vorticity equation, or alternatively (*e.g.* McIntyre 2000, Section 9) as a corollary of mass conservation together with Kelvin's circulation theorem applied to small constant- ϑ circuits. The neglect of MHD forces is much more of an open question, but, for what it is worth, the arguments of GM strongly justify such neglect in the downwelling branches of the tachocline ventilation circulation.

cancellation of strong positive and negative contributions from the northern and southern hemispheres respectively.

Owing to the positive-definiteness of the weighting factor b , the relation (8.4) imposes a severe constraint on the possible evolution of the global-scale Q distribution on each surface \mathcal{S} . We shall see that (8.4) is almost enough, by itself, to guarantee that layerwise-two-dimensional fluctuations about a mean state of solid rotation will behave anti-frictionally. Consistently with (8.4), one may picture Q as the amount per unit mass of a fictitious ‘PV substance’ composed of charged particles to which the stratification surfaces \mathcal{S} are completely impermeable. They are impermeable even if the motion is not adiabatic. Even if mass leaks across a surface \mathcal{S} , through thermal diffusion, the notional particles of ‘PV substance’ remain trapped on that surface (Haynes & McIntyre 1990). The ‘PV charge’ is conserved in the same way as electric charge. That is, pair production and annihilation are allowed, but no net charge creation or destruction. Just as $b dA d\vartheta$ is the mass element, $Q b dA d\vartheta$ is the charge element. The picture is consistent with (8.4) because the value, zero, of $\iint Q b dA$ cannot be changed by pair production and annihilation. Nor can it be changed by the advective rearrangement of the notional particles on each surface \mathcal{S} by any layerwise-two-dimensional motion.

A third key property of Q is its ‘invertibility’. This says that the isentropic distributions of Q , *i.e.* the distributions of PV values on the surfaces \mathcal{S} , contain nearly all the kinematical information about the layerwise-two-dimensional motion – whether or not MHD forces are significant. At each instant, to good approximation, one can ‘invert’ the PV field to get the velocity, pressure and density fields. The dynamical system is then completely specified by the PV inversion operator together with a single prognostic equation for the rate of change of Q , supplemented, if necessary, by a prognostic (induction) equation for any magnetic fields that may be present. The equation for Q can be $DQ/Dt = 0$ or an appropriate generalization, symbolically

$$DQ/Dt = \text{viscous, diabatic and MHD terms} . \quad (8.5)$$

The single time derivative reminds us that Rossby waves and other layerwise-two-dimensional motions, viewed in the rotating frame, are chiral: they notice the direction and sense of Ω_0 . The mirror-image motion is impossible.

All this is simplest to see in the limiting case of anelastic motion and infinitely heavy stratification, in which $N^2 \rightarrow \infty$ and $Ri \rightarrow \infty$. The surfaces \mathcal{S} become rigid and horizontal – horizontal in the billiard-table sense, with the sum of the gravitational and centrifugal potentials constant – and the

flow on each \mathcal{S} becomes strictly horizontal and strictly incompressible. Then $\mathbf{v} = \hat{\mathbf{r}} \times \nabla_{\mathcal{S}}\psi$ for some streamfunction ψ , and

$$Q = b^{-1}(f + \nabla_{\mathcal{S}}^2\psi) \quad (8.6)$$

with b strictly constant, where f is the vertical component of $2\Omega_0$ and $\nabla_{\mathcal{S}}$ and $\nabla_{\mathcal{S}}^2$ are the two-dimensional gradient and Laplacian on the surface \mathcal{S} . We may regard (8.6) as a Poisson equation to be solved for ψ when Q is given. Solving it is a well defined, and well behaved, operation provided that the given Q field satisfies the integral relation (8.4) on each \mathcal{S} . Symbolically,

$$\mathbf{v} = \hat{\mathbf{r}} \times \nabla_{\mathcal{S}}\psi \quad \text{with} \quad \psi = \nabla_{\mathcal{S}}^{-2}(bQ - f). \quad (8.7)$$

This expresses PV invertibility in the limiting case. Notice that the limiting case is degenerate in that the radial coordinate r enters the problem only as a parameter. There is no derivative $\partial/\partial r$ anywhere in the problem, either in the Laplacian or in the material derivative $D/Dt = \partial/\partial t + \mathbf{v} \cdot \nabla$, \mathbf{v} now being strictly horizontal. Not only is the motion layerwise-two-dimensional, but the layers are completely decoupled. There is, therefore, an implicit restriction on magnitudes of $\partial/\partial r$, *i.e.* an implicit restriction on the smallness of vertical scales, as the limit is taken.

More realistically, when N^2 and Ri are large but finite, $\partial/\partial r$ reappears in the problem and brings back vertical coupling. The motion remains layerwise-two-dimensional in the sense that the notional ‘PV particles’ move along each stratification surface \mathcal{S} , but the surfaces themselves are no longer quite horizontal, nor quite rigid. All the vertical coupling comes from the PV inversion operator. The two-dimensional inverse Laplacian in (8.7) is replaced by an inverse elliptic operator that resembles a three-dimensional inverse Laplacian when a stretched vertical coordinate Nr/f is used.

Here one has to make tradeoffs between accuracy and simplicity. The simplest though least accurate inversion operator is that arising in the standard ‘quasi-geostrophic theory’, an asymptotic theory for large Ri and $f \neq 0$, valid away from the equator. MHD forces are still absent from the inversion and, if significant at all, enter the problem only through the prognostic equation (8.5). The operator $\nabla_{\mathcal{S}}^2$ becomes $\nabla_{\mathcal{S}}^2 + \rho^{-1}\partial_r(\rho f^2 N^{-2}\partial_r)$. We may expect this to be a self-consistent approximation if Alfvén speeds are of the order of $|\mathbf{v}|$ or less. Notice that for tachocline eddies of horizontal scale 10^5 km, say, the vertical coupling extends over a vertical scale $\sim (f/N) \times 10^5$ km $\sim 0.004 \times 10^5$ km at latitude 45° , fairly small in comparison with a tachocline thickness of 0.13×10^5 km.

Some idea of what is involved in constructing more accurate inversion operators can be gained from the recent work of Ford *et al.* (2000) and

Mobehalhojeh & Drischel (2001 & refs.) and summarized in a recent review of mine (2001); see also the earlier discussion by Hoskins *et al.* (1985). Subtle generalizations of the notions of ‘geostrophic balance’ and ‘magnetostrophic balance’ are involved, and there are ultimate limitations on the accuracies attainable and on good mathematical behaviour, owing to phenomena such as Lighthill radiation, equatorial inertial instabilities, symmetric-baroclinic or Høiland instabilities, and magneto-rotational or Chandrasekhar–Fricke–Balbus–Hawley instabilities.

Before going further with the theory, let us take note of what layerwise-two-dimensional motion looks like in the real-world example that has been the most thoroughly studied, the Earth’s stratosphere. There, thanks to today’s observing systems, we can see many of the associated phenomena in remarkable detail, including conspicuous examples of Rossby-wave propagation.

8.4 A glimpse of the Earth’s stratosphere

Figure 8.1 presents two snapshots of the stratosphere, showing at a spatial resolution of a few degrees latitude the effects of layerwise-two-dimensional motion on two stratification surfaces \mathcal{S} . These surfaces lie at altitudes of about 31 and 37 km. An animated version can be seen on my website.† The figure is reproduced by courtesy of Dirk Offermann, Martin Riese, and the other scientists involved in the CRISTA space-based remote-sensing project; see Riese *et al.* (2002). The quantity shown is the mixing ratio $X_{\text{N}_2\text{O}}$ of a biogenic chemical tracer, nitrous oxide, that is destroyed photochemically on a timescale of years but resupplied, across the stratification surfaces \mathcal{S} from the troposphere below, on the same timescale of years, by a global-scale circulation called the Brewer–Dobson circulation. This is a stratospheric counterpart of the tachocline ventilation circulation. In the stratosphere the upwelling branch of the circulation is in the tropics; therefore $X_{\text{N}_2\text{O}}$ values are highest there. White areas are data gaps.

The layerwise-two-dimensional motion has far greater horizontal velocities than the Brewer–Dobson circulation, and far shorter timescales of days to weeks. On such timescales $X_{\text{N}_2\text{O}}$ is a near-perfect passive tracer, indeed material invariant, $\text{D}X_{\text{N}_2\text{O}}/\text{D}t = 0$ to good approximation. Thus, apart from the overall pole-to-equator gradient, the patterns seen in Figure 8.1 are shaped almost exclusively by the layerwise-two-dimensional motion.‡

† In colour, at www.atm.damtp.cam.ac.uk/people/mem/papers/LIM/index.html#crista-movie

‡ The observational resolution is enough for our purposes, though there must in reality be invisible fine-grain detail, such as the filamentary, cream-on-coffee patterns found in recent high-resolution observational and modelling studies of stratospheric flows at lower altitudes (*e.g.* Norton 1994, Waugh & Plumb 1994, Waugh *et al.* 1994, Appenzeller *et al.* 1996).

Each snapshot shows similar features, notably the well-mixed region (medium gray) on the right, with nearly uniform tracer values, sandwiched between relatively isolated polar and tropical airmasses having very different tracer values, with steep gradients in transition zones between. It is clear from the animated version and from numerical model simulations, which produce generically similar tracer distributions (*e.g.* Norton 1994), that the layerwise-two-dimensional motion is causing strong mixing on each stratification surface \mathcal{S} in an extensive midlatitude region sandwiched between the polar and tropical airmasses. A long tongue of tropical air is being drawn eastward past the tip of South America (light gray, inner band on the left) and marks the early stages of a typical mixing event, in which air is visibly recirculating within the midlatitude region at the instant shown. This horizontal recirculation is conspicuous in the animation. Because of the strong mixing, it is reasonable to regard the motion as fully turbulent, in the layerwise-two-dimensional sense, in middle latitudes.

However, the motion as a whole has not only its turbulent aspect but also the wavelike aspect anticipated theoretically. This too is conspicuous in the animated version of Figure 8.1, which shows the long axis of the central, elongated dark region rotating clockwise through an angle of about 70° longitude in 5 days, 10–15 August 1997, relative to the Earth. The central region marks the core of the ‘polar vortex’, characterized by large negative values of Q . Because of the approximate material invariance of Q , it behaves like an advected tracer on the short timescales of the layerwise-two-dimensional motion, and has a distribution somewhat like that of $X_{\text{N}_2\text{O}}$ apart from an additive constant.

The rate at which the long axis rotates is determined by a competition between the mean winds – which broadly speaking blow clockwise, at speeds of the order of 80 m s^{-1} , about nine times faster than 70° in 5 days – and a wave propagation mechanism that powerfully rotates the long axis anticlockwise relative to the air. This is the Rossby-wave or vorticity-wave mechanism.† The phase progression is necessarily one-way (here anticlockwise, or retrograde, relative to the air), as a consequence of the chirality associated with the single time derivative in equation (8.5).

As is well known, the Rossby-wave mechanism operates whenever Q has a mean gradient $\partial\bar{Q}/\partial\theta$ on stratification surfaces \mathcal{S} , such as the gradient associated with the global-scale polarization – the positive-to-negative, pole-to-pole variation in Q values due to the rotation of the whole system, Ω_0 say,

† As usual, terminology contradicts historical precedent. Carl-Gustaf Rossby was one of the greatest pioneers in atmospheric science, and his memory deserves special honour, but the wave mechanism was noted decades earlier by Kelvin and Kirchhoff, in special cases at least.

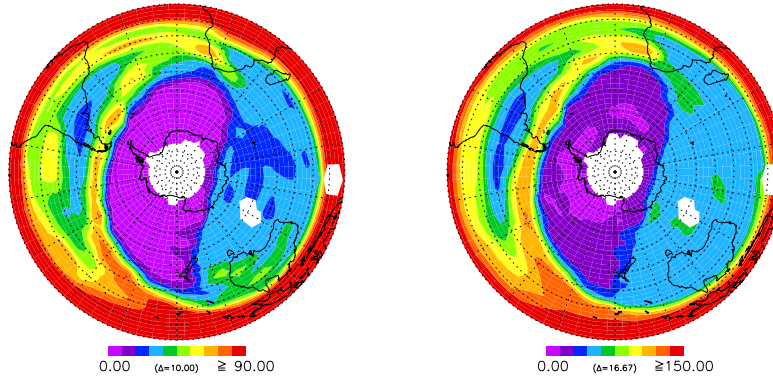


Fig. 8.1. Nitrous oxide (N_2O) mixing ratios $X_{\text{N}_2\text{O}}$ observed at two stratospheric altitudes on 11 August 1997 by the CRISTA infrared spectrometer, from Riese *et al.* (2002). White areas are data gaps. On Rossby-wave timescales of days and weeks N_2O is an accurate passive tracer, though destroyed photochemically on Brewer–Dobson timescales of years. In the right half of each picture $X_{\text{N}_2\text{O}}$ values increase equatorward nearly monotonically or stepwise monotonically (being nearly constant over the large medium gray regions on the right). Polar-vortex values (dark central regions) are close to zero, and tropical values are high, imported from the troposphere by the Brewer–Dobson upwelling. **At left and right respectively:** pressure-altitudes are 4.64 hPa and 10 hPa, roughly 37 km and 31 km; ranges of mixing ratios in parts per billion by volume are 0–90+ and 0–150+ with contour intervals 10 and 16.67, where ‘+’ signifies that maximum values may slightly overshoot the plotted range; the light band in the subtropics highlights the ranges 60–70 and 100–116.67 ppbv. CRISTA (CRyogenic Infrared Spectrometers and Telescopes for the Atmosphere) detects a number of chemical species through their infrared spectral signatures and is a large (1350 kg) helium-cooled instrument flown from the Space Shuttle.

which must here be taken to be somewhat faster than the rotation of the solid Earth. North–south material displacements across that gradient give rise to a pattern of fluctuating Q anomalies on the surfaces \mathcal{S} that alternate in sign downstream, every 90° of longitude in the case of Figure 8.1. Inversion of that pattern of Q anomalies to obtain the fluctuating velocity field produces north–south velocities that lag north–south displacements by a quarter wavelength in longitude, implying one-way phase propagation with highest \bar{Q} values on the right, *i.e.* retrograde phase propagation.

To check this qualitative picture in the simplest possible way using the standard Rossby–Haurwitz wave theory, take the limiting case (8.7), linearize the prognostic equation $\text{D}Q/\text{D}t = 0$ for small disturbances Q' , ψ' , \mathbf{v}' about a mean state of solid rotation Ω_0 , regard each stratification surface \mathcal{S} as precisely spherical and look for disturbances with complex amplitude \hat{Q} and spherical-harmonic structure $Q' = \text{Re}\{\hat{Q}P_n^m(\cos\theta)\exp(im\phi - i\omega t)\}$.

The linearized prognostic equation is

$$\frac{\partial Q'}{\partial t} + \frac{v_\theta'}{r} \frac{\partial \bar{Q}}{\partial \theta} = 0, \quad (8.8)$$

with $\partial \bar{Q}/\partial \theta = -2\Omega_0 b^{-1} \sin \theta$, $b = \text{constant}$, and $\Omega_0 = |\Omega_0|$. PV inversion reduces to $\psi' = \nabla_S^{-2}(bQ')$, hence $\hat{\psi} = -r^2 b \hat{Q}/\{n(n+1)\}$, with $\hat{\psi}$ the complex amplitude of ψ' , *i.e.*, $\psi' = \text{Re}\{\hat{\psi} P_n^m(\cos \theta) \exp(im\phi - i\omega t)\}$. Noting that $v_\theta' = -(r \sin \theta)^{-1} \partial \psi'/\partial \phi$ and that $\partial/\partial \phi = im$, we have

$$\omega = -\frac{2\Omega_0 m}{n(n+1)}. \quad (8.9)$$

This illustrates the qualitative picture sketched above, including the one-way propagation associated with chirality – the single power of ω coming from the single time derivative. Because the angular phase velocity $\omega/m < 0$, the phase propagation is retrograde and the meridional disturbance velocity v_θ' , with complex amplitude $\propto -im\hat{\psi}$, lags the displacement, with complex amplitude $\propto -im\hat{\psi}/(-i\omega) = m\omega^{-1}\hat{\psi}$, by a quarter wavelength in longitude.

More realistic models of stratospheric Rossby waves must take account of the turbulent mixing in middle latitudes. The mixing has an obvious qualitative effect: it weakens the PV gradient $\partial \bar{Q}/\partial \theta$ in middle latitudes and strengthens it at the subtropical edge of the midlatitude mixing region (outermost light band, clearest on the right of Figure 8.1) and at the polar edge bounding the vortex core. This characteristic reshaping of the $\bar{Q}(\theta)$ profile is suggested schematically by the cartoon on the left of Figure 8.2, in which y denotes northward distance in arbitrary units, $y \propto -\theta$, in a midlatitude slab model. The dashed and heavy lines represent the $\bar{Q}(y)$ profiles before and after mixing. The middle graph presents the corresponding $\bar{Q}(y)$ profiles in an actual numerical experiment, to be referred to shortly. Thus, in more realistic models, the quasi-elastic resilience associated with the Rossby-wave mechanism tends to be concentrated in transition zones of steep Q gradients, also marked by steep $X_{\text{N}_2\text{O}}$ gradients, lying between the tropical, midlatitude and polar airmasses. The same quasi-elastic resilience is part of why the three airmasses are chemically so distinct, with little mixing between them, a phenomenon seen again and again by stratospheric researchers and much studied because of its significance for ozone-layer chemistry. ‘Shear sheltering’ is also involved (Jukes & McIntyre 1987; Hunt & Durbin 1999).

For our purposes, however, the most important point of all is that the layerwise-two-dimensional mixing in middle latitudes owes its existence to the Rossby waves. In this respect the situation illustrated in Figure 8.1 is fundamentally similar to the ocean-beach situation, in which the turbulence

in the ocean-beach surf zone owes its existence to surface gravity waves. That is part of what I meant by the assertion that in the dynamical regimes under discussion ‘there is no such thing as turbulence without waves’.

The midlatitude mixing occurs for well-understood reasons associated with flow unsteadiness, hyperbolic points, and so on – a chaotic-advection kinematics very much tied, in this case, to the wave propagation, as analysed in detail by, for instance, Polvani & Plumb (1992). We may say that the turbulent mixing is intimately, and inseparably, part of the wavemotion. It is therefore reasonable to consider these stratospheric Rossby waves to be *breaking* waves. For this reason, the midlatitude mixing region is often called the ‘stratospheric surf zone’.

Numerical experiments in which the initial condition is axisymmetric, and in which Rossby waves are then excited somehow, commonly produce surf zones like that seen in Figure 8.1 (*e.g.* Norton 1994). The formation of surf zones is a very robust feature of such experiments, almost regardless of how chaotic or regular the waves, as such, happen to be. In the Earth’s stratosphere the Rossby-wave fields can on occasion be fairly regular, as in the case of Figure 8.1, or, more typically in the northern-hemispheric winter, rather more chaotic.

A fundamentally similar phenomenon of surf-zone formation was demonstrated long ago in the idealized numerical experiments of Rhines, in a classic paper entitled ‘Waves and turbulence on a beta-plane’ (Rhines 1975). The designations ‘Rossby-wave breaking’ and ‘stratospheric surf zone’ can be justified in a very general way, from wave–mean interaction theory (*e.g.* McIntyre & Palmer 1985), having regard to Kelvin’s circulation theorem. This has application to most if not all non-acoustic wave types.

In the Rossby-wave case the whole conceptual picture is illustrated by a specific model of wave breaking in a certain parameter limit, known as the Stewartson–Warn–Warn model, in which the surf zone is narrow and the interplay between the wavelike and turbulent dynamics can be precisely and comprehensively described using matched asymptotic expansions (Haynes 1989 & refs.). This is based on the midlatitude slab model in the limiting case (8.7), and has provided a set of detailed examples including that from which Figure 8.2b is derived. The interplay works both ways, at leading order: not only do the waves create the turbulence – again justifying the idea of ‘wave breaking’ – but the turbulence, in turn, strongly influences the wavefield, and in particular the systematic correlations between v_{θ}' and v_{ϕ}' that are significant for horizontal momentum transport. The wavefield, through the PV inversion operator, senses the horizontal rearrangement of PV substance by the turbulence within the surf zone.

8.5 Turbulence requires waves

There is an alternative, independent justification for the assertion that in the dynamical regimes under discussion ‘there is no such thing as turbulence without waves’. The justification follows simply and directly from PV invertibility, involving no restriction to special parameter regimes, and no reliance on particular mathematical techniques such as that of matched asymptotic expansions.

We assume the existence of turbulence without waves, and show that this leads to a contradiction. More precisely, consider a layerwise-two-dimensional PV mixing event like those depicted in Figure 8.2a,b, in which the PV profile $\bar{Q}(\theta)$ or $\bar{Q}(y)$ is changed by a finite increment $\delta\bar{Q}$ within some finite mixing region $y_1 < y < y_2$ or $\theta_1 < \theta < \theta_2$, in such a way as to respect the integral relation (8.4). The dashed lines show the initial $\bar{Q}(y)$ profile. In the case of the cartoon in Figure 8.2a, the profile of $\delta\bar{Q}(y)$ is a simple N-shape, having negative slope within the mixing region.

Imagine that the mixing somehow takes place without any wave mechanism being involved. The PV invertibility principle says that when the \bar{Q} profile changes then the mean velocity profile must change too, by $\delta\bar{v}_\phi$ say. In the limiting case (8.7) the relevant inversion is trivial, b being constant; for instance in the slab model it is simply

$$\delta\bar{v}_\phi(y) = \int_y^\infty \delta\bar{Q}(\tilde{y}) b d\tilde{y} . \quad (8.10)$$

For the N-shaped $\delta\bar{Q}(y)$ profile, the shape of $\delta\bar{v}_\phi(y)$ is a simple parabola. For the $\delta\bar{Q}(y)$ profile implied by Figure 8.2b, the shape of $\delta\bar{v}_\phi(y)$ is qualitatively the same, the parabola-like shape given by the right-hand plot, Figure 8.2c.

These mean flow changes show a net momentum deficit. Notice that $\int_{y_1}^{y_2} \delta\bar{v}_\phi(y) dy = \int_{y_1}^{y_2} y \delta\bar{Q}(y) b dy$ (integrating by parts): the total momentum change, ignoring a constant factor ρ , is equal to the first moment of $\delta\bar{Q}(y)$. This is negative for the N-shaped $\delta\bar{Q}(y)$ profile. The first moment, and the momentum change itself, both have unambiguous meanings in virtue of the integral relation (8.4), which implies that $\int_{y_1}^{y_2} \delta\bar{Q}(y) b dy = 0$ in the present limiting case (8.7), with b constant. So the momentum deficit is indeed a deficit whenever $\delta\bar{Q}(y)$ is such that the mixing event was indeed a mixing event, in the sense of weakening the gradient of \bar{Q} within the mixing region $y_1 < y < y_2$.

The argument just presented can easily be generalized from the slab

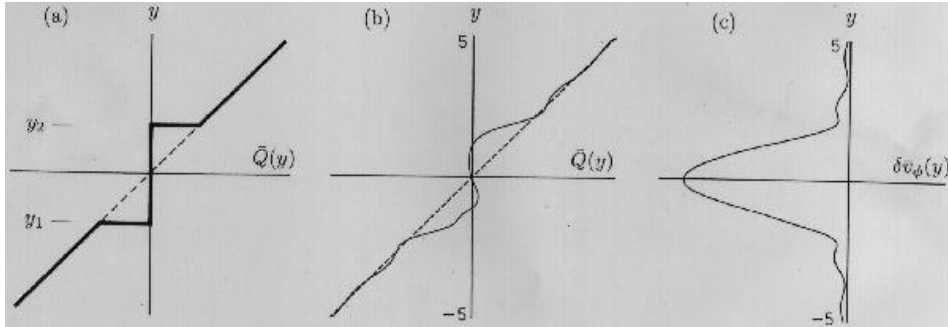


Fig. 8.2. Demonstration that rearrangement of PV substance by layerwise-two-dimensional mixing on a stratification surface \mathcal{S} , within some latitude band $y_1 < y < y_2$, must entail momentum transport outside the band hence wavelike as well as turbulent fluctuations. (This follows from PV invertibility, and does not require accurate material invariance of Q .) The quantitative examples in plots (b) and (c) are by courtesy of P. H. Haynes (personal communication); for full mathematical details see Killworth & McIntyre (1985) and Haynes (1989). Plot (a) shows idealized \bar{Q} distributions before and after mixing; (b) shows the same in an accurate slab-model simulation, using $DQ/Dt = 0$ together with the inversion (8.7); (c) shows the resulting mean momentum change, given by equation (8.10), whose profile would take a simple parabolic shape in the idealized case corresponding to (a).

geometry to the spherical geometry, replacing equation (8.10) by

$$\delta \bar{v}_\phi(\theta) = r (\sin \theta)^{-1} \int_0^\theta \delta \bar{Q}(\tilde{\theta}) b \sin \tilde{\theta} d\tilde{\theta}. \quad (8.11)$$

We can also remove the restriction to the limiting case (8.7), reverting to finite N^2 and Ri . In the most accurate versions it is necessary to redefine the mean \bar{Q} around latitude circles as a weighted ‘isentropic’ mean at constant ϑ , *i.e.* following a stratification surface \mathcal{S} , with weighting function b , so as to respect the integral relation (8.4). It is then convenient to switch to ϑ as the vertical coordinate, as discussed under the heading ‘isentropic coordinates’ in the atmospheric-science literature (*e.g.* Andrews *et al.* 1987). The main conclusion, that layerwise-two-dimensional PV mixing produces a momentum or angular momentum deficit, still holds good.†

It follows that – whatever the purely turbulent (Austausch) stresses that might be involved – such turbulent stresses cannot satisfy the momentum budget on their own. This point was made long ago by Stewart & Thomson (1977) who, however, used it to claim that turbulent mixing scenarios like

† In fact the conclusion holds exactly on each surface \mathcal{S} in any thought experiment in which the initial and final states are axisymmetric. The vertical coupling represented by the ∂_r term in quasi-geostrophic theory is incapable, by itself, of transporting absolute angular momentum, and so never enters the calculation.

those of Figures 8.2a,b cannot be realized. This overlooked the possibility that ‘the problem of turbulence’ might have a wavelike aspect, allowing momentum to be exchanged between the mixing region and its surroundings.

To summarize, then, the implication in reality is that wave-induced momentum transport, not confined to mixing regions such as $y_1 < y < y_2$ in Figure 8.2, is an essential part of the picture – essential to making sense of the fluid dynamics as a whole. The turbulent mixing scenarios can in fact be realized, but only in the presence of waves, which, in the stratospheric case at least, are chiefly Rossby waves.

The Stewartson–Warn–Warn model played an important role in developing the conceptual framework just sketched, by illustrating, with great precision, how everything works and fits together in a particular set of idealized thought experiments. We may note too that the same thought experiments provide especially clear examples of anti-frictional behaviour.

In each case a shear flow $\bar{v}_\phi \propto y$ is disturbed by monochromatic Rossby waves generated by an undulating boundary located at positive y , outside the domain of Figure 8.2. The graphs plotted in Figures 8.2b,c come from one such thought experiment but are qualitatively similar to those from all the others. In each case the surf zone or mixing zone surrounds the location $y = 0$, a so-called ‘critical line’ where, by definition, \bar{v}_ϕ coincides with the longitudinal phase speed of the Rossby waves. The phase speed is retrograde relative to the mean flow throughout $y > 0$, so that Rossby-wave propagation is possible there. The fluid behaviour within the surf zone is complicated and chaotic in most cases; for detailed examples and for a definitive and thorough analysis see Haynes (1989). The behaviour is anti-frictional because the momentum transport that accounts for the momentum deficit in the surf zone, equation (8.10) and Figure 8.2c, is everywhere against the mean momentum gradient $\partial\bar{v}_\phi/\partial y > 0$, through a positive correlation between v'_y and v'_ϕ .

More generally, equation (8.10) and (8.11) show that in any thought experiment starting with solid rotation on a given stratification surface \mathcal{S} , such as the solid rotation observed below the Sun’s tachocline, the formation of mixing regions like that in Figure 8.2 will drive the system away from solid rotation. This general point is reinforced by the integral relation (8.4). Because b is positive definite, (8.4) tells us at once that the only way to mix Q to homogeneity on a stratification surface \mathcal{S} is to make Q zero everywhere – a fantastically improbable state on a planet rotating like the Earth, or in a star rotating like the Sun. Since real Rossby waves do break, and do mix Q , they must be expected to do so imperfectly, mixing more strongly in some places than in others and producing the characteristic spatial inhomogeneity

that always seems to be observed, as illustrated by Figure 8.1. Again, the effect is to drive the system away from solid rotation.

To be sure, one can imagine a thought experiment in which the air on and near the stratification surface \mathcal{S} begins by rotating solidly, and then has its angular velocity uniformly reduced by breaking Rossby waves. The PV mixing would have to be distributed in just such a way as to give a uniformly reduced pole-to-pole latitudinal profile of Q , keeping it precisely proportional to $\cos\theta$. But the tailoring of a Rossby-wave field to do this would be a more delicate affair than standing a pencil on its tip, and the natural occurrence of such a wave field would be another fantastically improbable thing. A sufficient reason for its improbability is the positive feedback associated with PV mixing. As soon as some region begins to be mixed, PV gradients and Rossby quasi-elasticity are weakened, facilitating further mixing. Conversely, PV gradients are tightened at the edges of the mixing regions, tending to inhibit mixing there, as evidenced for instance by the steep $X_{\text{N}_2\text{O}}$ gradients at the edges of the surf zone in Figure 8.1.

Nonmagnetic laminar spindown would also produce differential rotation. This was part of why GM argued that an internal magnetic field in the Sun is not merely possible but actually inevitable – the only way to account for the observed near-solid rotation in the radiative, heavily stratified interior.

8.6 Concluding remarks

The general arguments of Section 8.5 are enough to show that in heavily stratified systems there is no such thing as turbulence without waves, and hence that stratification-constrained horizontal eddy viscosities are implausible, if MHD effects are negligible. The general arguments leave open the question of which waves. The reason for focusing here on Rossby waves rather than gravity waves, for instance, is that the timescale of the tachocline ventilation circulation, $\sim 10^6\text{y}$ (see SZ and GM), while long in comparison with that of the sunspot cycle, $\sim 10\text{y}$, is short in comparison with the Sun’s lifetime and spindown time, $\sim 10^{10}\text{y}$. A number of published and unpublished estimates of gravity-wave amplitudes in the Sun’s interior, based on the reasonable hypothesis that gravity waves are generated mainly by the overlying convection zone, point to momentum transports that could be significant on spindown timescales but fall far short of being significant on tachocline ventilation timescales.

Acoustic waves are still weaker, for this purpose, leaving only the question of Alfvén and other MHD waves. GM’s arguments justify the neglect of MHD effects in the downwelling branches of the tachocline ventilation circu-

lation, outside the midlatitude band of upwelling. The downwelling firmly confines the large-scale interior magnetic field to the tachopause and below, as GM showed with the help of an appropriate magnetic boundary-layer theory. Rapidly alternating solar-cycle fields could be carried downward from the top of the tachocline but should diffusively self-annihilate far faster than the 10^6 y timescale of the downwelling.

In the midlatitude upwelling branch, the magnetic boundary-layer theory fails. Superficial layers of the interior field must be fed into the tachocline then into the convection zone. Exactly how that happens is uncertain, and no detailed model is available as yet, though it must be the main means whereby the interior field leaks out, contributing to the decay from its primordial state – a scenario that fits well with the fact that interior magnetic diffusion times for the largest possible scales, *i.e.* for a simple internal dipole, are comparable to the Sun’s lifetime. In the tachocline’s upwelling branch the presence of large-scale magnetic field may give rise to significant angular momentum transport, either directly via Alfvénic elasticity as field lines are sheared out, or via MHD waves. Or the upwelling may itself be locked into solid rotation. All we know so far is that mass conservation dictates that the upwelling branch must exist, and that the physics of thermal diffusion and the pattern of vertical shear in the tachocline inferred from helioseismic inversions (*e.g.* Thompson *et al.* 1996, Kosovichev 1997, Schou *et al.* 1998) dictates, through a very robust ‘thermal wind balance’, *i.e.* through large-scale hydrostatic and cyclostrophic balance, that the upwelling must indeed be taking place in middle latitudes (SZ, GM). The upwelling branch remains the biggest missing piece of the jigsaw puzzle put together in GM.

The ‘gyroscopic pumping’ of the tachocline ventilation circulation, and of the stratospheric Brewer–Dobson circulation, is a well understood process in stratified, rotating fluid dynamics and has been discussed extensively elsewhere (*e.g.* McIntyre 2002 & refs.). Persistent westward or eastward forces pump fluid persistently poleward or equatorward, respectively, through Coriolis-induced turning. Ekman pumping is the special case in which the east–west forces are frictional forces near a boundary; in the stratosphere the forces are wave-induced. For the Sun the important points to note are (1) that the only process able to provide east–west forces of sufficient strength is the three-dimensional turbulence in the convection zone, through its Reynolds and Maxwell stresses, (2) that the resulting ventilation circulation tends to burrow downward, (3) that the burrowing can be stopped only by the interior magnetic field, and (4) that a complete model of convection-zone differential rotation must take account of the thermal structure of the tachocline induced by the ventilation circulation, hotter in

downwelling and cooler in upwelling regions, with its thermal-wind link to differential rotation. The implied differential rotation must be continuous with that in the convection zone, again by thermal-wind balance. It follows that the tachocline determines the differential rotation at the base of the convection zone – not *vice versa* – and that the convection zone reacts back on the tachocline by reshaping the Reynolds and Maxwell stresses and the consequent gyroscopic pumping. To my knowledge there has been no effort, so far, to construct a model that captures this two-way coupling.

With the inevitability of a poloidal magnetic field in the interior below the tachopause, we may expect magneto-rotational instabilities to be potentially significant in the interior as well as in the tachocline’s upwelling branch. As pointed out in Balbus & Hawley (1991 & refs., especially Fricke 1969), magneto-rotational instabilities should operate in stellar interiors with poloidal magnetic fields, in such a way as to prevent $\bar{\Omega}$ from decreasing outwards from the rotation axis. This plus Ferraro’s law of isorotation could clamp the upwelling and most of the interior into solid rotation – except in the ‘polar pits’ at the hairy-sphere defects in the horizontal magnetic field at the tachopause, which as GM pointed out are the only locations where the gyroscopically pumped tachocline circulation can burrow down far enough to burn lithium and beryllium. Notice, incidentally, how the arguments of Section 8.5 are vitiated by the poloidal magnetic field: PV advection is nullified by MHD effects on the right-hand side of equation (8.5). There is no longer any tendency to form PV mixing regions!

If the interior is clamped into solid rotation almost everywhere, it hardly needs saying that there are strong implications both for helioseismic inversion and for understanding primordial spindown. Furthermore, older speculations such as mine of 1994, about QBO-like torsional oscillations in stellar interiors, would now appear to be ruled out.

Acknowledgements I thank Martin Riese for Figure 8.1, Peter Haynes for Figures 8.2b,c, Pascale Garaud for sharing unpublished results, Jørgen Christensen-Dalsgaard, Rosanne Gough, Mike Thompson, and Sylvie Vauclair for organizing a superb conference and for inviting me to take part, Ed Spiegel and Nigel Weiss for stimulating conversations on astrophysics over the years, and last, but certainly not least, Douglas Gough for further such stimulus and encouragement and for his indomitable spirit, sense of fun, and passion for good science. My research owes much to atmospheric-science and fluid-dynamics colleagues too numerous to mention and was supported by the Natural Environment Research Council, the Isaac Newton Institute for Mathematical Sciences, and a SERC/EPSC Senior Research Fellowship.

References

- Andrews, D. G., *et al.*, 1987. *Middle Atmosphere Dynamics*. Academic, 489 pp.
- Appenzeller, C., *et al.*, 1996. *J. Geophys. Res.*, **101**, 1435–1456.
- Balbus, S. A. & Hawley, J. F., 1991. *Astrophys. J.*, **376**, 214–222.
- Baldwin, M. P., *et al.*, 2001. *Revs. Geophys.*, **39**, 179–229.
- Brillouin, L., 1925. *Annales de Physique*, **4**, 528–586.
- Elliott, J. R. & Gough, D. O., 1999. *Astrophys. J.*, **516**, 475–481.
- Ford, R., *et al.*, 2000. *J. Atmos. Sci.*, **57**, 1236–1254.
- Fricke, K., 1969. *Astr. Astrophys.*, **1**, 388–398.
- Gough, D. O. & McIntyre, M. E., 1998. *Nature*, **394**, 755–757. [GM]
- Haynes, P. H., 1989. *J. Fluid Mech.*, **207**, 231–266.
- Haynes, P. H. & McIntyre, M. E., 1990. *J. Atmos. Sci.*, **47**, 2021–2031.
- Hoskins, B. J., *et al.*, 1985. *Q. J. Roy. Meteorol. Soc.*, **111**, 877–946.
- Hunt, J. C. R. & Durbin, P. A., 1999. *Fluid Dyn. Res.*, **24**, 375–404.
- Jeffreys, H., 1933. In *Selected Papers on the Theory of Thermal Convection*, ed. B. Saltzman, 1962. New York, Dover, 200–210.
- Jukes, M. N. & McIntyre, M. E., 1987. *Nature*, **328**, 590–596.
- Killworth, P. D. & McIntyre, M. E., 1985. *J. Fluid Mech.*, **161**, 449–492.
- Kosovichev, A. G., 1997. *Sol. Phys.*, **170**, 43–61.
- Lorenz, E. N., 1967: *The Nature and Theory of the General Circulation of the Atmosphere*. Geneva, World Meteorol. Org., 161 pp.
- McIntyre, M. E., 1994. In *The Solar Engine and its Influence on the Terrestrial Atmosphere and Climate* (Vol. **25** of NATO ASI Subseries I, Global Environmental Change), ed. E. Nesme-Ribes; Heidelberg, Springer, 293–320.
- McIntyre, M. E., 2000. In *Perspectives in Fluid Dynamics: A Collective Introduction to Current Research*, ed. G. K. Batchelor, H. K. Moffatt, M. G. Worster; Cambridge, University Press, 557–624.
- McIntyre, M. E., 2001. In *Proc. IUTAM Limerick Symposium on Advances in Mathematical Modelling of Atmosphere and Ocean Dynamics*, ed. P. F. Hodnett; Dordrecht, Kluwer Academic Publishers, 45–68.
- McIntyre, M. E., 2002. In *Meteorology at the Millennium*, ed. R. P. Pearce; London, Academic Press and Royal Meteorol. Soc., 283–305.
- McIntyre, M. E. & Palmer, T. N., 1985. *Pure Appl. Geophys.*, **123**, 964–975.
- Mohebalhojeh, A. R. & Dritschel, D. G., 2001. *J. Atmos. Sci.*, **58**, 2411–2426.
- Norton, W. A., 1994. *J. Atmos. Sci.*, **51**, 654–673.
- Plumb, R. A. & McEwan, A. D., 1978. *J. Atmos. Sci.*, **35**, 1827–1839.
- Polvani, L. M. & Plumb, R. A., 1992. *J. Atmos. Sci.*, **49**, 462–476.
- Rhines, P. B., 1975. *J. Fluid Mech.*, **69**, 417–443.
- Riese, M., *et al.*, 2002. *J. Geophys. Res.*, **107**(D23), # 8179, pp. CRI 7-1 to 7-13.
- Schou, J., *et al.*, 1998. *Astrophys. J.*, **505**, 390–417.
- Spiegel, E. A. & Zahn, J.-P., 1992. *Astron. Astrophys.*, **265**, 106–114. [SZ]
- Stewart, R. W. & Thomson, R. E., 1977. *Proc. Roy. Soc. Lond.*, **A354**, 1–8.
- Thompson, M. J., *et al.*, 1996. *Science*, **272**, 1300–1305.
- Waugh, D. W. & Plumb, R. A., 1994. *J. Atmos. Sci.*, **51**, 530–540.
- Waugh, D. W., *et al.*, 1994. *J. Geophys. Res.*, **99**, 1071–1078.